Journal of Chromatography A, 1218 (2011) 3130–3139

Contents lists available at ScienceDirect

Journal of Chromatography A

journal homepage: www.elsevier.com/locate/chroma

Achieving high peak capacity production for gas chromatography and comprehensive two-dimensional gas chromatography by minimizing off-column peak broadening

Ryan B. Wilson, W. Christopher Siegler, Jamin C. Hoggard, Brian D. Fitz, Jeremy S. Nadeau, Robert E. Synovec*

Department of Chemistry, Box 351700, University of Washington, Seattle, WA 98195-1700, USA

ARTICLE INFO

Article history:
Available online 4 January 2011

Keywords:
Peak capacity production
Gas chromatography
Comprehensive
High speed

ABSTRACT

By taking into consideration band broadening theory and using those results to select experimental conditions, and also by reducing the injection pulse width, peak capacity production (i.e., peak capacity per separation time) is substantially improved for one dimensional (1D-GC) and comprehensive two dimensional (GC × GC) gas chromatography. A theoretical framework for determining the optimal linear gas velocity (the linear gas velocity producing the minimum *H*), from experimental parameters provides an in-depth understanding of the potential for GC separations in the absence of extra-column band broadening. The extra-column band broadening is referred to herein as off-column band broadening since it is additional band broadening not due to the on-column separation processes. The theory provides the basis to experimentally evaluate and improve temperature programmed 1D-GC separations, but in order to do so with a commercial 1D-GC instrument platform, off-column band broadening from injection and detection needed to be significantly reduced. Specifically for injection, a resistively heated transfer line is coupled to a high-speed diaphragm valve to provide a suitable injection pulse width (referred to herein as *modified injection*). Additionally, flame ionization detection (FID) was modified to provide a data collection rate of 5 kHz. The use of long, relatively narrow open tubular capillary columns and a 40 °C/min programming rate were explored for 1D-GC, specifically a 40 m, 180 μm i.d. capillary column operated at or above the optimal average linear gas velocity. Injection using standard auto-injection with a 1:400 split resulted in an average peak width of ~1.5 s, hence a peak capacity production of 40 peaks/min. In contrast, use of modified injection produced ~500 ms peak widths for 1D-GC, i.e., a peak capacity production of 120 peaks/min (a 3-fold improvement over standard auto-injection). Implementation of modified injection resulted in retention time, peak width, peak height, and peak area average RSD%'s of 0.006, 0.8, 3.4, and 4.0%, respectively. Modified injection onto the first column of a GC × GC coupled with another high-speed valve injection onto the second column produced an instrument with high peak capacity production (500–800 peaks/min), ~5-fold to 8-fold higher than typically reported for GC × GC.

1. Introduction

One-dimensional gas chromatography (1D-GC) has been an important method of analysis for complex mixtures of volatile and semi-volatile organic compounds for several decades. Much of the current research effort focuses on refining the general practice of 1D-GC to decrease the analysis time, and/or to produce instrumental and computational advances that allow the analysis of increasingly complex samples. Underlying all of these research efforts is the development of strategies to increase the peak capacity production [1] (i.e., the number of peaks that fit within a given separation time in the chromatogram at a specified resolution). The pursuit of high peak capacity production involves decreasing the width of chromatographic peaks, because the smaller the peak width then more peaks will fit in a given separation time. The width of peaks observed in GC is the sum of the on-column and off-column contributions, where on-column broadening is broadening that occurs to the analyte peak while it is in the column, and off-column broadening is broadening due to injection, detection, column connections, electronics, etc. Typically, on-column broadening is minimized by applying GC theory to determine optimal pressure and flow conditions for a given column, while off-column broadening is addressed via improvements to instrumentation.

Of particular interest in this report is off-column band broadening due to injection, and reducing it in order to enhance peak

* Corresponding author. Fax: +1 206 685 8665.
E-mail address: synovec@chem.washington.edu (R.E. Synovec).

0021-9673/$ – see front matter © 2011 Elsevier B.V. All rights reserved.
doi:10.1016/j.chroma.2010.12.108

capacity production. The standard 1D-GC auto-injector on various commercial instruments injects a sample pulse typically ~1 s wide. Researchers have devoted a significant amount of attention to reducing the injection pulse width, with most techniques falling into two groups: mechanical valves and thermal based focusing devices. Single high-speed diaphragm valves are capable of injections of ~15 ms [2], while a dual diaphragm valve injection system has been reported that resulted in injection pulses as small as 0.5 ms [3]. However, in the development of an injection system, it is important to optimize, as much as is possible, the representativeness of the sample injected onto the column. As will be shown herein for a valve-based injection system, separation can occur in the transfer line between the GC inlet and the valve when oven temperatures are low, as is typically the case at the beginning of a temperature programmed separation [4]. Thermal injection techniques, on the other hand, are unaffected by oven temperatures and have been demonstrated to be capable of 10 ms injection pulses [5]. The narrow peaks resulting from the narrow injection pulses should, in principle, result in high peak capacity production rates for even the fastest separations.

Another source of band broadening is non-uniform oven temperatures and temperature programming rates. Early reports of high-speed 1D-GC separations were almost exclusively isothermal, due to inadequate temperature programming capabilities. Commercial instruments are now available with conductive heating systems, allowing programming rates in excess of 10 °C/s with rapid cool down rates for reducing total cycle time. Direct resistive heating of metal columns has also been reported with rates in excess of 200 °C/s [4,6]. Despite these advances, the vast majority of 1D-GC instruments in laboratories today temperature program via a traditional convection oven. For example, the standard Agilent 6890 is limited to a maximum program rate of 40 °C/min over typical temperature ranges (e.g. 50–250 °C). Deviation from linear program rates can occur at temperatures above 175 °C and with faster program rates [7]. With these instrumental limitations, standard 1D-GC methods are generally limited to temperature program rates of 30 °C/min or less. In a recent report by Leonard et al. [7], the application of various temperature programming rates available in conventional 1D-GC instruments to high-speed separations was studied, concluding that longer (25 m) columns resulted in the best peak capacity production values.

Band broadening can further be minimized by optimizing other experimental parameters, including the column dimensions (length and inside diameter (i.d.)), stationary phase thickness, and carrier gas linear velocity. Recent research in isothermal high-speed 1D-GC theory outlined expected peak widths for various column dimensions when operated at the theoretical minimum plate height, H, in the absence of external sources (i.e., off-column) of band broadening. According to Reid and Synovec [8], all columns of common lengths (1–100 m) and i.d. range (50–530 μm) are capable of producing peak widths ranging from less than 600 ms (for long 530 μm i.d. columns) to as little as 0.6 ms (for short 50 μm i.d. columns), for an unretained analyte ($k = 0$). However, typical 1D-GC methods often result in peak widths of 1 s or more. Indeed, it is common to see peaks on the order of 2 s wide at the base for 1D-GC [9–11] and typically 6–20 s wide in the first dimension for comprehensive two-dimensional gas chromatography (GC × GC) [12,13]. Peak broadening of this magnitude can be due to a variety of reasons: intentional implementation of non-optimal column separation conditions, off-column sources of broadening, or more likely, a combination of the above. Regardless of the source, the result of the broadening is decreased peak capacity production from the instrument.

In this context, GC × GC, pioneered by Phillips and co-workers in the early 1990s, represents another tactic for increasing the overall peak capacity production of a GC instrument [14]. For GC × GC, two separation columns with sufficiently orthogonal stationary phases are connected in series by a suitable injection modulation interface. Effluent from the first column is collected and injected onto the second column by the modulation interface. The ideal peak capacity, $n_{c,GC\times GC}$, of such a GC × GC instrument is the product of the peak capacities of each separation dimension [9]. Since GC × GC separations should be completed in the same amount of time as an equivalent 1D-GC separation, the addition of a second column should in principle provide a dramatic improvement in peak capacity production. However, as pointed out by Blumberg et al. [15], the typical practice of slowing down the column 1 separation to allow the long column 2 separations required by wide modulation pulses gives peak capacity production rates that are between ~50 and 150 peaks/min, which as we shall demonstrate herein is much lower than what is achievable. For example, with 6 s wide peaks on column 1, using a modulation period of 2 s to achieve reasonably comprehensive separations [16], and with peak widths of ~200 ms on column 2, the peak capacity production is 100 peaks/min.

In this current report, the theoretical framework for on-column band broadening previously reported [8] was extended to temperature programmed 1D-GC. Utilizing this extended theory, a 40 m long column with a 180 μm i.d. was selected for use with a relatively fast temperature program available from an Agilent 6890 GC. The modified injection system (following the auto-injector), composed of a heated transfer line leading to a single diaphragm valve, was experimentally characterized and implemented to minimize off-column band broadening from the injection process. Based on the extended theory for on-column band broadening, instrumental parameters were optimized to provide evenly distributed peak widths throughout the separations achieved, resulting in significantly increased peak capacity production. The benefits of the modified injection system are demonstrated on both 1D-GC and GC × GC instruments.

2. Theory

For a given resolution ($R_s = 1$, herein) the theoretical peak capacity for a 1D-GC separation, $n_{c,GC}$ is given by

$$n_{c,GC} = \frac{{}^1t_R - {}^1t_M}{{}^1w_b} \tag{1}$$

where ${}^1t_R$ is the separation run time on column 1 (and could be viewed as the last retained peak at the end of the separation), ${}^1t_M$ is the dead time on column 1 and ${}^1w_b$ is the average peak width throughout the temperature programmed 1D chromatogram. Requiring higher resolution (e.g., 1.5–2) will decrease the peak capacity proportionally. For a GC × GC separation $n_{c,GC\times GC}$ is ideally the product of the peak capacity for each dimension

$$n_{c,GC\times GC} = \frac{{}^1t_R - {}^1t_M}{{}^1w_b} \cdot \frac{{}^2t_R}{{}^2w_b} \tag{2}$$

where ${}^2t_R$ is the separation run time on column 2 (suggesting that ${}^2t_R$ is sufficiently greater than ${}^2t_M$ and could be viewed as the last retained peak at the end of that separation, or alternatively wrap-around is allowed to fully utilize the column 2 modulation period P_M), and ${}^2w_b$ is the average peak width throughout the column 2 separation. To calculate the 1D-GC peak capacity production, $n_{c,GC}$ is simply divided by ${}^1t_R - {}^1t_M$,

$$\frac{n_{c,GC}}{{}^1t_R - {}^1t_M} = \frac{1}{{}^1w_b} \tag{3}$$

For the GC × GC case, where ${}^2t_R$ is equivalent in this sense to the modulation period, P_M, and thus the modulation ratio, M_R, is

equal to ${}^1w_b$ divided by P_M, the resulting GC × GC peak capacity production is [17]

$$\frac{n_{c,\mathrm{GC\times GC}}}{{}^1t_R - {}^1t_M} = \frac{{}^2t_R}{{}^1w_b \cdot {}^2w_b} = \frac{P_M}{{}^1w_b \cdot {}^2w_b} = \frac{1}{M_R \cdot {}^2w_b} \tag{4}$$

If the peak widths on column 1 can be maintained going from 1D-GC to GC × GC, the expected theoretical increase in relative peak capacity production is then simply calculated from

$$\frac{n_{c,\mathrm{GC\times GC}}}{n_{c,\mathrm{GC}}} = \frac{{}^1w_b}{M_R \cdot {}^2w_b} = \frac{P_M}{{}^2w_b} \tag{5}$$

Not surprisingly, a longer modulation period combined with narrow peaks on column 2 produces the largest relative increase in peak capacity production. However, this result is deceiving because it obscures the relationship between modulation period and column 1 peak capacity production, where a longer modulation period in a GC × GC separation may necessitate wider peaks on the column 1 to obtain comprehensive data, than would otherwise be obtained in an optimized 1D-GC separation.

From Eqs. (3) and (5), it is apparent that it is possible to increase peak capacity and peak capacity production by decreasing the peak width. To determine the lower limits for peak widths (and thus the upper limits for peak capacity production) for a column of given dimensions, it is necessary to further understand on-column band broadening. Excluding off-column sources of band broadening, the on-column band broadening, H, for an analyte with a retention factor of k as derived by Golay is given by

$$H = \frac{2D_{G,o}jf}{\bar{u}} + \frac{1 + 6k + 11k^2}{96(1+k)^2}\frac{d_c^2\bar{u}f}{D_{G,o}j} + \frac{2kd_f^2\bar{u}}{3(1+k)^2D_L} \tag{6}$$

where k is the retention factor of the analyte, d_c is the i.d. of the capillary, d_f is the thickness of the stationary phase film, $D_{G,o}$ is the diffusion coefficient of the analyte in the gas phase at the outlet of the column, j and f are gas compression correction factors, D_L is the diffusion coefficient of the analyte in the stationary phase, and $\bar{u}$ is the average linear velocity of the carrier gas. With the reduced pressure, P, given as the ratio of the inlet and outlet pressures P_i/P_o, the well-known James–Martin gas compressibility factor (j) and the Giddings gas compressibility factor (f) are defined:

$$j = \frac{3}{2}\frac{P^2 - 1}{P^3 - 1} \tag{7}$$

$$f = \frac{9(P^4 - 1)(P^2 - 1)}{8(P^3 - 1)^2} \tag{8}$$

For unretained analytes (such as methanol at 90 °C under experimental conditions studied herein) k is equal to 0. The Golay equation (Eq. (6)) in such a situation, simplifies to

$$H = \frac{2D_{g,o}jf}{\bar{u}} + \frac{d_c^2\bar{u}f}{96D_{g,o}j} \tag{9}$$

Defining the optimal average linear gas velocity, $\bar{u}_{\mathrm{opt}}$, as that occurring at the minimum value of H, i.e., H_{min}, we set the derivative of Eq. (9) to zero and solve for $\bar{u}$, yielding an expression for $\bar{u}_{\mathrm{opt}}$

$$\bar{u}_{\mathrm{opt}} = \frac{\sqrt{192}D_{g,o}j}{d_c} \tag{10}$$

providing a relationship between the optimum average linear gas velocity and the i.d. of the capillary. However, Eq. (10) does not clearly indicate the dependence and interrelationship of $\bar{u}_{\mathrm{opt}}$ on the capillary length. To elucidate this relationship it is necessary to begin with the relationship between $\bar{u}_{\mathrm{opt}}$ and experimentally relevant parameters. Another useful expression for $\bar{u}$ in terms of the column length, L, carrier gas viscosity, η, pressure at the column outlet, P_o, and other parameters previously defined is given by [18]

$$\bar{u} = \frac{d_c^2P_o}{64\eta L}(P^2 - 1)j \tag{11}$$

When $\bar{u} = \bar{u}_{\mathrm{opt}}$ for a given set of conditions, the reduced pressure, P, is referred to as $P_{@\mathrm{opt}}$. Thus, Eq. (11) is set equal to Eq. (10). Solving for $P_{@\mathrm{opt}}$ gives the following,

$$P_{@\mathrm{opt}} = \sqrt{64\sqrt{192}\frac{D_{g,o}\eta L}{d_c^3P_o} + 1} \tag{12}$$

Given typical values for $D_{G,o}$, η and P_o, one can readily calculate $P_{@\mathrm{opt}}$ for a column with given dimensions L and d_c. Substituting this expression for $P_{@\mathrm{opt}}$ back into Eq. (7) yields j, which can subsequently be substituted into Eq. (10), providing the following relationship

$$\bar{u}_{\mathrm{opt}} = \frac{3}{2}\frac{\sqrt{192}D_{g,o}}{d_c}\left(\frac{P_{@\mathrm{opt}}^2 - 1}{P_{@\mathrm{opt}}^3 - 1}\right) \tag{13}$$

where $\bar{u}_{\mathrm{opt}}$ is related to $P_{@\mathrm{opt}}$, $D_{G,o}$ and d_c. Note that $\bar{u}_{\mathrm{opt}}$ is also implicitly related, through Eq. (12), to L, P_o, and η. Additionally, a simplified expression for H_{min} is obtained by substituting Eq. (10) into Eq. (9)

$$H_{\mathrm{min}} = \frac{fd_c}{\sqrt{12}} \tag{14}$$

Now that both $\bar{u}_{\mathrm{opt}}$ and H_{min} are defined, additional useful information about the separation, i.e., hold-up time, efficiency and peak width, can be determined. The efficiency, N, of the separation is conventionally given by

$$N = 16\left(\frac{t_R}{w_b}\right)^2 = \frac{L}{H} \tag{15}$$

with the analyte retention time, t_R, and peak width at the base, w_b, in units of time. Of particular interest is the peak width because of its inverse relationship with peak capacity production. Since the retention time is related to the dead time, t_M, of the separation by the retention factor k as follows

$$k = \frac{t_R - t_M}{t_M} \tag{16}$$

and, since the dead time t_M in terms of L and $\bar{u}$ is $t_M = L/\bar{u}$, combining Eqs. (15) and (16), solving for w_b while setting $k = 0$ yields the following relationship,

$$w_b = \frac{4}{\bar{u}}\sqrt{HL} \tag{17}$$

At experimental conditions where $\bar{u} = \bar{u}_{\mathrm{opt}}$ and $H = H_{\mathrm{min}}$ the optimum peak width, $w_{b@\mathrm{opt}}$, is

$$w_{b@\mathrm{opt}} = \frac{4}{\bar{u}_{\mathrm{opt}}}\sqrt{H_{\mathrm{min}}L} \tag{18}$$

This $w_{b@\mathrm{opt}}$ is the peak width at the base of an unretained analyte ($k = 0$) at $\bar{u}_{\mathrm{opt}}$ due only to on-column band broadening, without off-column band broadening.

Herein, the modified injection system (heated transfer line with a single high-speed diaphragm valve following the autoinjector) will be demonstrated to minimize injection broadening, the high-speed FID electrometer to minimize detection band broadening, while the theory presented above provides a point of comparison for evaluating our experimental efforts to minimize

Table 1
Compounds included in the complex GC × GC test mixture. Listed in elution order with boiling point.

Elution order	Compound	Boiling point (°C)
1	1-Propanol	97
2	Benzene	80
3	1-Heptene	94
4	2-Pentanol	116
5	Heptane	98
6	1-Heptyne	100
7	1-Pentanol	137
8	Toluene	111
9	Octane	126
10	Chloro-benzene	132
11	1-Cholor-hexane	135
12	Ethyl-benzene	136
13	DMMP	181
14	3-Heptanone	149
15	2-Heptanone	151
16	*o*-Oxylene	144
17	Nonane	151
18	Bromo-benzene	156
19	1-Bromo-hexane	155
20	Mesitylene	165
21	3-Octanone	165
22	Tert-butylbenzene	170
23	Decane	174
24	1-Br-heptane	108
25	Butylbenzene	182
26	1-Undecene	193
27	Undecane	196
28	Methyl caprylate	240
29	1,3,5-Trichlorobenzene	209
30	1-Bro-octane	202
31	Naphthalene	218
32	1-Dodecane	214
33	Dodecane	215
34	Tridecane	234
35	Methyl decanoate	224
36	Tetradecane	254
37	*n*-Pentadecane	270
38	Hexadecane	287
39	Heptadecane	303
40	Pristane	296
41	Octadecane	305
42	Nonadecane	330
43	Dibutylphthalate	340
44	Eicosane	344

band broadening in relation to standard auto-injection with the GC.

3. Experimental

3.1. Reagents and chemicals

All chemicals were reagent grade or higher: methanol (J.T. Baker, Phillipsburg, NJ, USA), anisole and octanol (Aldrich, Fairlawn, NJ, USA), and tridecane (Alfa Aesar, Ward Hill, MA, USA). A 4 component test mixture was prepared from these neat solvents with approximately equal concentration by volume of each. The four solvents (components) were chosen to span a boiling point range of 65 °C (methanol) to 234 °C (tridecane) to evaluate the modified injection system. Polar analytes were included in the mixture to demonstrate that modified injection is effective across compound classes. Gasoline was also used as a demonstration of a complex sample, and was obtained from a local gas station. The compounds in the complex mixture used in the GC × GC experiment are listed in the order of elution in Table 1. Boiling points for each analyte were found in the CRC handbook of Chemistry and Physics [19]. The mixture was prepared by mixing neat analytes with sufficient concentration of each to be able to see each analyte signal.

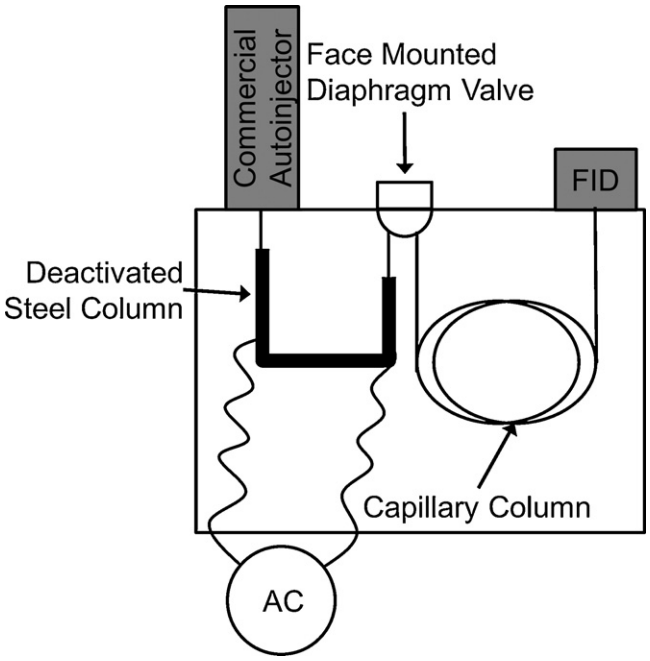

Fig. 1. Diagram of the Agilent 6890 GC with the modified injection system. Changes include mounting a high-speed diaphragm valve in the GC and a high-speed electrometer board for the FID. The valve inlet is connected to the instrument inlet by a 15 cm resistively heated, deactivated steel column transfer line. The transfer line is electrically insulated from the GC by short lengths of deactivated fused silica column.

3.2. Instrumentation

All chromatograms were obtained using an Agilent 6890 gas chromatograph with an auto-injector controlled by ChemStation software (Agilent Technologies, Palo Alto, CA, USA) modified as illustrated in Fig. 1. The Agilent FID was supplemented with a custom electrometer that was built in-house and capable of providing data acquisition at a rate of 20 kHz. This electrometer was interfaced to a National Instruments data acquisition board (model PCI-MIO-16XE-50, National Instruments, Austin, TX, USA) and the resulting data was collected using a LabVIEW 8 (National Instruments) program written in-house at a rate of 5 kHz. The GC instrument was modified to use a diaphragm valve (VICI, Valco Instruments Co. Inc., Houston, TX, USA), fitted with a 10 μl sample loop for injecting a sample volume onto the column. The single valve injection system presented by Hope et al. [2] was refined by face mounting the valve as described by Sinha et al. [20], allowing for a wider range of oven temperatures (comfortably to 250 °C). For samples containing higher boiling point compounds (the complex test mixture described in Table 1), the injection system was further refined by switching the ports flowing into the valve (carrier gas and inlet reversed) and the outlet ports (the column and vent reversed). In this configuration the "load" and "inject" positions are effectively switched [2]. The valve was timed to 'load' for a short period after auto-injection and then 'inject' for the remainder of the separation, allowing the sample loop to completely purge during the temperature program. With this valve configuration the sample volume injected is determined by the volume of the sample loop, not the time the valve is open. For the GC × GC experiments a second diaphragm valve, with a 1.3 μl sample loop was added to repeatedly collect and inject the effluent from column 1 onto column 2 at a specified modulation period. Valve timing and actuation were controlled using the same LabVIEW program described above. For the modified injection system, sample was delivered from the GC inlet to the diaphragm valve via a 15 cm length of deactivated steel column with a 250 μm i.d. (UADTM-5, Quadrex Corporation, Wool-

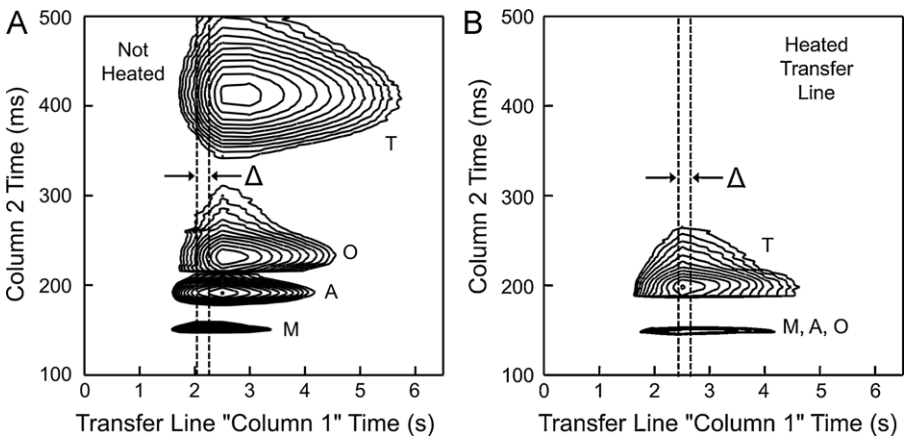

Fig. 2. (A) 2D separation of a four analyte test mixture in a GC × GC instrumental configuration using a 15 cm deactivated steel transfer line for the first dimension and a 1.4 m MXT-5 column as the second dimension. The retention order is methanol (M), anisole (A), octanol (O), and tridecane (T). Both dimensions had 414 kPa of absolute head pressure. Analytes were injected onto the second dimension column using 15 ms pulses every 0.5 s. The oven temperature was 150 °C. The 15 ms time pulse Δ is illustrated as it depicts the pulse of sample injected using the modified injection system in Fig. 1. (B) The 2D behavior of the modified injection system is observed. The same instrumental parameters as A were used except that ~12 V were applied to the first dimension to resistively heat the transfer line.

bridge, CT, USA). This steel column transfer line was electrically insulated from the GC using two short lengths of deactivated fused silica column, also with 250 μm i.d. (10079, Restek, Bellefonte, PA, USA). The fused silica sections of the transfer line were coupled to the steel column using steel column unions with a 250 μm i.d. bore (VICI). A variable autotransformer (Staco Energy Products, Dayton, OH, USA) supplied ~12 V of alternating current to the transfer line via three high temperature electrical leads placed on opposite ends of the steel column unions, hence producing a heated transfer line at ~250 °C (measured with an infrared thermometer) leading to the diaphragm valve with the 10 μl sample loop.

3.3. Chromatographic experiments

To characterize the heated transfer line performance, 2D-like separations were completed using the heated transfer line described above as column 1, and a 1.4 m MXT-5 Silicosteel column (Restek) with a 180 μm i.d. and a 0.4 μm film thickness (5% phenyl/95% dimethyl polysiloxane) as column 2. For these experiments the inlet was operated under a 5:1 split at 414 kPa absolute while the head pressure on the column 2 was also 414 kPa absolute. These separations were performed with a modulation period of 500 ms and a 15 ms injection pulse width. At an average volumetric flow of ~1 μl/ms, 15 μl are flushed through the sample loop during injection, ensuring the 10 μl sample loop is sufficiently purged for the purpose of the modified injection system study. The oven was held at 150 °C throughout the run.

When utilizing the transfer line for injections in both the 1D-GC and GC × GC configurations, the inlet was operated with a split of 5:1 at a relative pressure of 207 kPa. In both GC and GC × GC studies the oven was held at 90 °C for 0.5 min, programmed from to 250 °C at 40 °C/min, and held at 250 °C for 0.5 min. 1D-GC separations were completed using a 40 m Rtx-5 column (Restek) with a 180 μm i.d. and a 0.4 μm film thickness (5% phenyl/95% dimethyl polysiloxane). Valve injections were 15 ms wide unless otherwise noted in the text.

GC × GC separations were performed, using the same 40 m Rtx-5 column with a 180 μm i.d. for column 1. For column 2, a 2 m D5 trigonal tricationic ionic liquid column with a 100 μm i.d. and 0.08 μm film thickness was used. This novel stationary phase, developed by Payagala et al. [21], consists of a tri (2-hexanamido) ethylamine core surrounded by propylphosphonium cationic moieties. The modulating valve injected 15 ms pulses every 200 ms, fully evacuating the contents of the 1.3 μl sample loop. For clarity, absolute pressure at the head of each column is specified for each separation in the text.

3.4. Theoretical calculations

All calculations were completed for columns of various lengths, L, and i.d., d_c, holding other parameters constant as specified. All calculations used H_2 as the carrier gas and, for the sake of brevity, using an analyte retention factor of $k = 0$. The diffusion coefficient of a typical analyte in the gas phase at the outlet of the column, $D_{G,o}$, was estimated for a temperature at the beginning of the temperature program (90 °C). An analyte with a relatively low boiling point, eluting with a $k = 0$ at 90 °C, such as methanol, will have a $D_{G,o} \sim 0.7\ cm^2/s$ (approximate). Viscosity of the carrier gas, η, was calculated for each temperature based on a fit to experimental data and is accurate for temperatures from 20 °C up to 400 °C and pressures around 101 kPa (the pressure dependence of viscosity is sufficiently small). The outlet of the column was assumed to be at an ambient pressure of 101 kPa.

4. Results and discussion

4.1. Evaluation of heated transfer line

In order to evaluate the modified injection system for making single injections for 1D-GC, it was initially configured in a "GC × GC mode," with the resistively heated transfer line as "column 1" making repeated injections onto a short, narrow column as column 2. An isothermal separation of the four component test mixture is shown in Fig. 2A. Note that the four analytes have different retention times in the transfer line (column 1) dimension, indicating that even though the transfer line is a deactivated steel column, sufficient retention occurs if the transfer line is not heated significantly above the oven temperature of 150 °C. The dotted lines in Fig. 2A demonstrate the volume sampled by a typical valve injection, defining Δ. In Fig. 2A we see the proportions of each analyte in the sample volume injected by the diaphragm valve onto column 2 are not sufficiently constant over time, i.e., as Δ is tuned across the column 1 time axis. If the transfer line and high-speed valve are used for a single injection, the sample being injected onto column 2 at any given time is not consistently representative of the sample injected on the transfer line. In contrast, with resistive heating of the transfer line to 250 °C, as demonstrated in Fig. 2B, significantly reduces retention time differences in the transfer line dimension. Unexpectedly, resis-

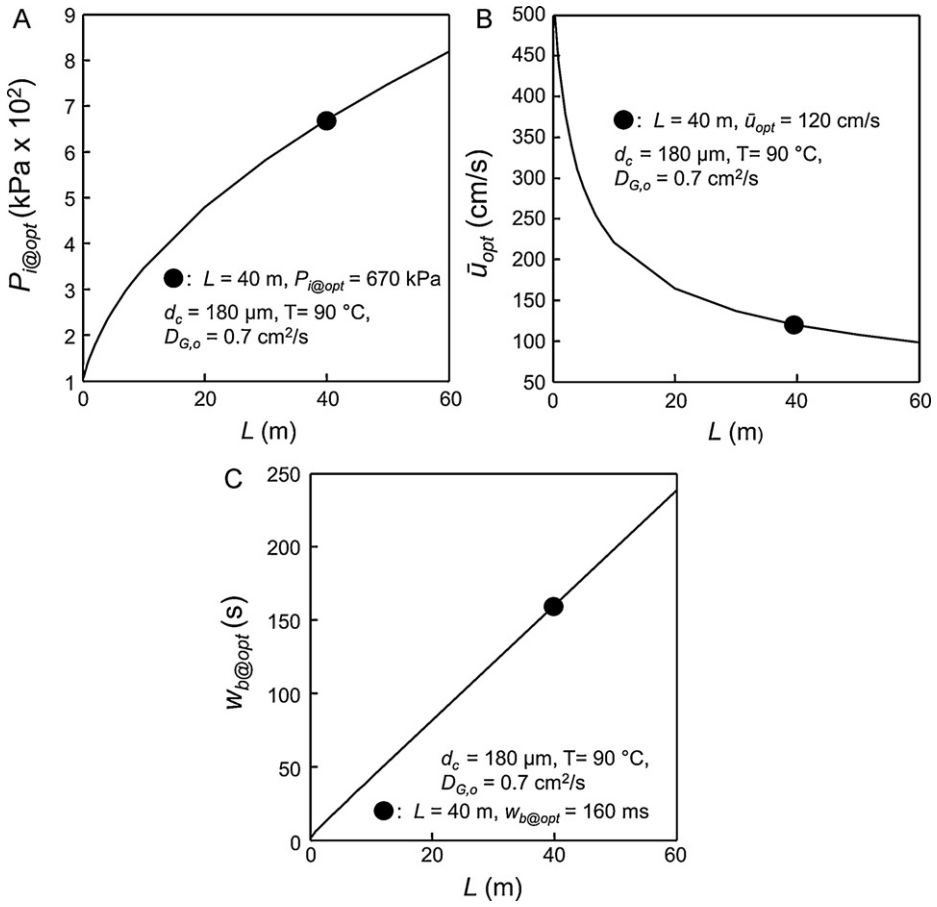

Fig. 3. (A) Plot of inlet pressure (P_i) at $\bar{u}_{opt}$ vs. column length (L) per Eq. (12) for a typical analyte eluting at 90 °C. (B) Plot of the optimum average linear gas velocity $\bar{u}_{opt}$ vs. column length L per Eq. (13) for the analyte described above. (C) Plot of the peak width at the base, $w_{b@opt}$ vs. the column length L per Eq. (18). The following parameters were used to calculate the values plotted: $k = 0$, H_2 carrier gas.

tive heating of the transfer line also appears to significantly reduce retention times on column 2, particularly for methanol, anisole, and octanol, which may be due to conductive heating of the metal capillary being used for column 2. A single injection from the valve at any time near the peak's center of mass (i.e., a 15 ms pulse could in principle be taken between 2 s and 4 s in Fig. 2B) defined by time width Δ provided a sample with analyte concentration proportions similar to those introduced by the auto-injector (i.e., with a controllable split), but with much less band broadening (as will be demonstrated). In addition to providing a narrow injection pulse, the diaphragm valve with the modified injection system also provides a split effect, by decreasing the amount of analyte injected on the column as compared to the amount of analyte leaving the instrument's inlet. Peak volume calculations indicate that if the time represented by Δ in Fig. 2B is a 15 ms pulse occurring 2.5 s after the initial injection, the diaphragm valve reduces the amount of analyte transferred from column 1 to column 2 by a factor of 160, i.e., equivalent to ~1:160 split. However, we shall see the 1:160 split with the modified injection system provides significantly less off-column band broadening as compared to the original auto-injection system at either a 1:200 or 1:400 split.

4.2. Column and instrument parameter selection

In our previous report [8] the above Theory provided analysts with broad insight into understanding how wide "in time" peaks could in principle be in 1D-GC (assuming no off-column band broadening). In that report, we applied the Theory to a single "typical" analyte with a single "typical" temperature while varying column dimensions. In this report, the theory is focused in its implementation by providing insight for column selection and instrument parameter selection for an unretained compound (methanol, with boiling point of 64.7 °C) eluting at the beginning of a temperature program (at 90 °C). We will compare and take note of the difference between taking the Theory approach provided herein relative to the commonly applied van Deemter plot approach.

A column with an i.d. of 180 μm was selected for this study because our previous theoretical work [8] had shown this i.d. would likely provide a high peak capacity production using a column length in the 20 m to 50 m range (with 40 m selected), which would also allow the maximum temperature ramp rate of 40 °C/min of the oven to be utilized. The absolute head pressure, P_i, required to obtain $\bar{u}_{opt}$ can be calculated for a variety of column lengths using Eq. (12). Indeed, $P_{i@opt}$ (the inlet pressure at $\bar{u}_{opt}$) for a column with 180 μm i.d. is plotted as a function of L in Fig. 3A. We selected $L = 60$ m as the longest length for the plots since this produces a $P_{i@opt}$ that is above 793 kPa, the pressure limit of most commercial GC instrumentation. Ideally, the column length and flow would result in a separation occurring on the same time scale as the oven ramp rate. For this study a column with a 180 μm i.d. and a length of 40 m was selected because the $P_{i@opt}$ of 670 kPa (dot in Fig. 3A) for the beginning of the temperature program would allow for further pressure programming during the temperature program to account for the increased carrier gas viscosity.

Calculating $P_{i@opt}$ allows j, H_{min}, and $\bar{u}_{opt}$ to be readily determined for the same experimental parameters. The dependence of $\bar{u}_{opt}$ on column length for 90 °C is shown in Fig. 3B (Eq. (13)). Subsequently, values for $w_{b@opt}$ can be calculated using Eq. (18). A plot

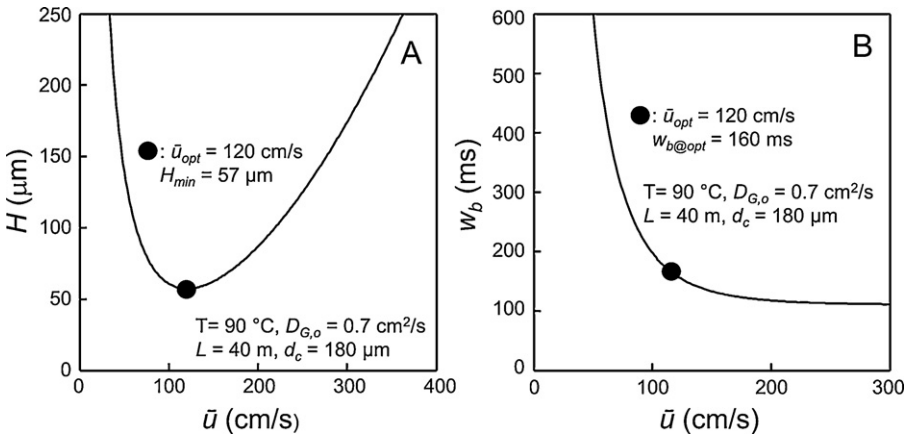

Fig. 4. (A) van Deemter plot of theoretical H vs. $\bar{u}$ for the same analyte as described in Fig. 3, calculated using Eq. (9). (B) Plot of theoretical w_b vs. $\bar{u}$ for the analyte described above, calculated using Eq. (18). The following parameters were used to calculate the values plotted: $k = 0$, H_2 carrier gas.

of $w_{b@\mathrm{opt}}$ as a function of L is shown in Fig. 3C (Eq. (18)). For the column chosen above (40 m long with a 180 μm i.d.), $\bar{u}_{\mathrm{opt}}$ is found to be 120 cm/s (Fig. 3B dot), meaning the dead time should be 33 s, while the optimal peak width is ~160 ms (Fig. 3C dot), for the unretained peak at the beginning of the temperature program starting at 90 °C.

This approach to band broadening theory incorporates the $\bar{u}_{\mathrm{opt}}$ from the van Deemter plots of a broad range of columns and instrument parameters into a succinct and simplified picture, useful to the general practitioner for selecting the appropriate column dimensions for a given application and evaluating experimental chromatographic data to determine the presence of off-column band broadening. On the other hand, the traditional van Deemter approach applies to one set of column dimensions, but illuminates the impact of changing linear gas velocities on the resulting separation. For instance, the van Deemter plot, with $k = 0$, at 90 °C is depicted in Fig. 4A, with the dot denoting the minimum plate height of 57 μm. The plot is created by calculating H for various values of $\bar{u}$ using Eq. (9). A plot of w_b as a function of $\bar{u}$ for the same analyte under the same conditions is given in Fig. 4B (Eq. (18)), with the width at the optimum linear flow velocity marked with a dot. From Fig. 4B it is clear that separations at linear flow velocities below the optimum can cause a significant increase in peak width, while there is a decrease in peak width above the optimum, encouraging the use of linear flow velocities at or above the optimum. The experimental realization of the peak widths in Fig. 4B is also dependent upon factors external to the column. The condition given above is that off-column band broadening is not included in the equations. To experimentally achieve peak widths as theoretically calculated above requires minimization of off-column band broadening due to injection, detection and other potential sources. For the column used in this study (40 m long, with 180 μm i.d.) and a temperature program beginning at 90 °C the theory indicates that the average peak width for early eluting analytes should be ~160 ms.

4.3. Peak width and peak capacity production

To demonstrate the benefit of minimizing injection band broadening, mixtures of the same four test analytes were analyzed using the column selected above and the instrument's maximum temperature program of 40 °C/min, using the two injection systems, standard auto-injection and modified injection. Injection via standard auto-injection, with relatively large splits (200:1 and 400:1), and an initial absolute column head pressure (310 kPa) selected according to Agilent's FlowCalc software resulted in chromatograms (Fig. 5A and B) in a separation time window of 180 s (from methanol to tridecane). Using Eq. (3) and an average peak width of 1.5 s gives a peak capacity production of 40 peak/min for a total peak capacity of 120 over this time window with the 200:1 split. The unretained peak (methanol) had a dead time of 88 s and a peak width at the base of 1.4 s, that translates into a chromato-

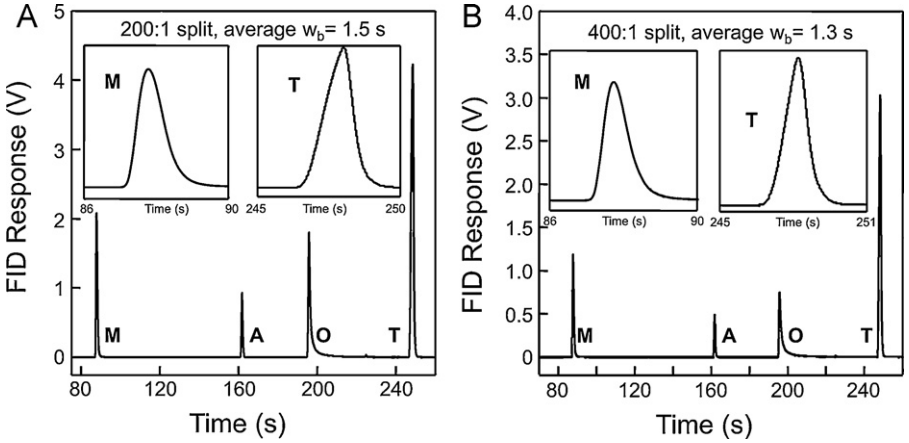

Fig. 5. (A) Separation of a four analyte text mixture utilizing a 40 m × 180 μm Rtx-5 column and the standard Agilent 6890 GC auto-injection. Here, a 0.5 μl of sample was injected with a 200:1 split. (B) The same separation as A except 0.5 μl of sample was injected with a 400:1 split. For both separations the oven was programmed from 90 to 250 °C at the maximum program rate of 40 °C/min. A constant volumetric flow at the column outlet of 1.3 ml/min was maintained by the instrument software. The retention order was methanol (M), anisole (A), octanol (O), and tridecane (T).

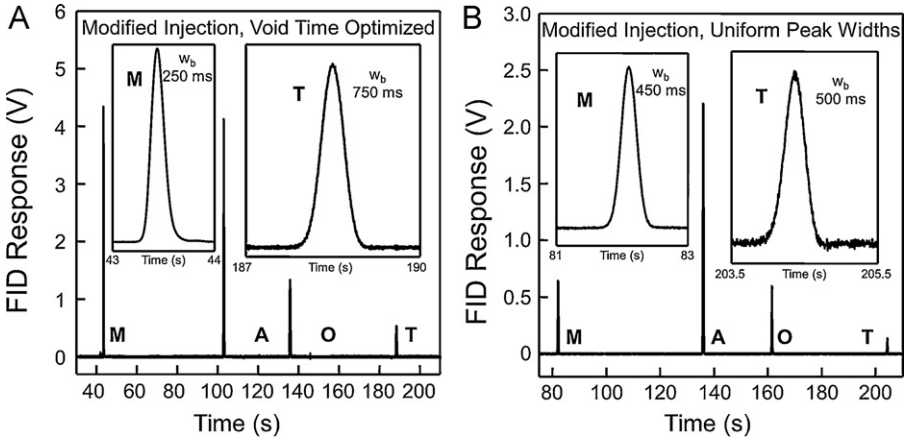

Fig. 6. (A) Separation of a four analyte test mixture utilizing a 40 m × 180 μm Rtx-5 column and the modified injection system (resistively heated transfer line with high-speed diaphragm valve). Sample was injected onto the column using 10 μl sample loop and a single 15 ms valve actuation. The auxiliary electronic pressure control was used to program the absolute head pressure on the column from 586 kPa to 793 kPa at a rate of 51.7 kPa/min during the temperature program. The same temperature program was used as in Fig. 5 resulting in the same retention order. (B) The same conditions as in A except the auxiliary electronic pressure control was used to program the absolute head pressure on the column from 310 kPa to 793 kPa at a rate of 121 kPa/min during the temperature program, resulting in essentially the same flow rate for the unretained methanol peak as in Fig. 5.

graphic efficiency of $N = 63{,}000$. Doubling the split to ratio 400:1 did not result in significantly better peak shape or width.

Using modified injection and an absolute column head pressure (586 kPa, programmed linearly to 793 kPa) similar to that recommended by theory, a second mixture of the same four components (albeit with different concentrations of the four components) was analyzed, resulting in a chromatogram in a separation window of 160 s (Fig. 6A). The peak width of the unretained analyte methanol was only 250 ms and approaches the 160 ms width predicted by theory (see Figs. 1C and 2B). Unfortunately, the peaks of analytes with larger retention times were progressively broadened to 750 ms for the last peak. Also notable is the reduction in tailing of octanol using the modified injection system as compared to the auto injector. Though the reason behind this improvement is not clear, it appears to be another benefit of the valve-based modified injection.

To facilitate comparison with the auto-injection separations in Fig. 5, the initial absolute column head pressure was reduced to 310 kPa, increasing the time each test analyte spent on the column and allowing each analyte to elute at a higher temperature and a lower retention factor. The resulting chromatogram, with nearly constant peak widths throughout the separation, is shown in Fig. 6B. The separation window was 130 s, with an average peak width of 500 ms, resulting in a peak capacity production of 120 peaks/min (Eq. (3)) and a total peak capacity of 260 over this time window. The separation in Fig. 6B represents a 3-fold increase in peak capacity production with a concurrent 2.2-fold increase in total peak capacity in 20% less separation time (compared to Fig. 5A or B). Additionally, one can objectively compare the band broadening of the unretained methanol peak in Fig. 6B to that in Fig. 5B, since both elute with approximately the same flow rate and temperature. The methanol peak width of 450 ms with a retention time of 82 s corresponds to an efficiency $N = 530{,}000$, an 8-fold improvement relative to the standard auto-injection with a 200:1 split. This is the most striking evidence for the reduction of the off-column band broadening, in conjunction with the evidence that when the column was run at optimum conditions for the unretained peak, that the peak width experimentally observed essentially matched that expected by theory applying Eq. (18) with $w_b \sim 160$ ms predicted for these conditions per Fig. 2C.

4.4. Reproducibility study

The four component test mixture separation was run in triplicate using the conditions in Fig. 6B. These replicates were used to evaluate the reproducibility of injections made by the heated transfer line, single high-speed diaphragm valve combination. The results are summarized in Table 2. For each analyte the retention time, peak width at the base, peak height and peak area were measured and the average reported with one standard deviation. For these measurements of interest, the RSD% for each analyte was averaged and reported. Considering the developmental nature of the modified injection system, values of 3.4% and 4% for the average relative standard deviation in peak height and peak area compare favorably to the 5% RSD% seen with traditional auto-injection (prior to applying an internal standard). The peak widths also show good precision indicating that valve actuation time is dependable. The relative standard deviation in analyte retention time is ~0.0006% which is very satisfactory for most applications, although more replicates for retention time would be needed to make a more rigorous assessment.

4.5. Application of optimized conditions to a gasoline sample

As a demonstration of the modified injection system under chromatographic conditions to achieve optimized and constant peak widths, the instrumental parameters from the separation in Fig. 6B were applied to a gasoline sample from a local service station.

Table 2
Reproducibility of retention time (t_R), peak width at the base, peak height and peak area, with ± one standard deviation, for the separation of the four analyte text mixture using the modified injection system (see Fig. 6B for representative chromatogram and experimental conditions).

	Methanol	Anisole	Octanol	Tridecane	%RSD
t_R (min)	1.3684 ± 0.0001	2.2668 ± 0.0001	2.6921 ± 0.0001	3.4060 ± 0.0002	0.006% ± 0.003
Peak width$_{@\ base}$ (ms)	459 ± 2	511 ± 5	498 ± 3	527 ± 7	0.8 ± 0.4
Peak height (V)	0.65 ± 0.01	2.11 ± 0.07	0.56 ± 0.03	0.13 ± 0.01	3.4 ± 1.9
Peak area	939 ± 7	3300 ± 130	880 ± 50	209 ± 14	4 ± 3

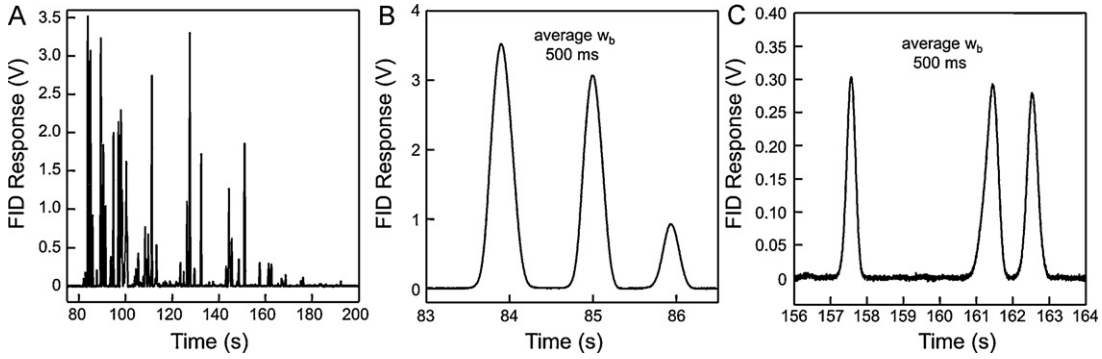

Fig. 7. Rapid separation of a gasoline sample utilizing the 40 m × 180 μm Rtx-5 column with the modified injection system. Sample was injected onto the column using 10 μl sample loop and a single 50 ms valve actuation. The same temperature and pressure program was used as in Fig. 6B.

Results for the gasoline sample separation in Fig. 7 were consistent with the previous optimized separation in Fig. 6B. The separation window was ~120 s. Peak widths of early eluting compounds are nearly the same width as those of late eluting compounds (~500 ms) resulting in a peak capacity production from Eq. (3) of ~120 peaks/min.

4.6. Application to a GC × GC separation

To further improve the peak capacity production of the instrument, the above 1D-GC configuration (Figs. 6B and 7) was coupled to a 2 m column 2 via a high-speed diaphragm valve modulator, face mounted in the GC wall to allow high temperature operation for GC × GC [20]. Fig. 8A demonstrates the potential of such a GC × GC instrument with the separation of a complex test mixture (Table 1) in a 4 min separation time window. Fig. 8B highlights a smaller region of the 2D chromatogram. Peak widths at 13% of the peak height are ~750 ms on column 1 for both early and late eluting compounds. The lowest contour of the chromatogram plot was chosen to be approximately 13% of the average peak height over that region of the chromatogram, corresponding to the peak width at the base (±2 standard deviations in time). On column 2 the peak widths range from 20 to 35 ms during the 200 ms modulation period. Hence, Eq. (18) gives peak capacity production rates ranging from 500 to 800 peaks/min. With the 200 ms modulation period, and column 1 peak widths of 750 ms, the modulation ratio was M_R of 3.8, which is quite adequate for a comprehensive GC × GC separations. Addition of the valve modulated column 2 resulted in back pressure from column 2 being applied to the primary column outlet every modulation, effecting both the dead time and peak widths on column 1. These issues were minimized by delaying the actuation of the modulator until just before the first peak eluted and increasing the initial head pressure on column 1. Fig. 8C is the 1D separation representation resulting from summing each second dimension separation in Fig. 8A. As the insert in Fig. 8C shows, peaks on the primary column are around 750 ms wide, resulting in a reduction of 1D peak capacity production to ~80 peaks/min (Eq. (17)). While the addition of the second column caused a 33% loss in peak capacity production from column 1, the high-speed modulation period and narrow peaks on column 2 increased the peak capacity production by a factor of ~10. Additionally, adding a polar ionic liquid column 2 to the non-polar column 1 provides excellent selectivity for the separation. The peaks eluting between 130 s and 160 s on column 1 that are not resolved in the 1D representation in Fig. 8C are resolved in the GC × GC separation of Fig. 8B. It is interesting to note that this GC × GC configuration is designed around an initially optimized primary column separation, and then utilizing the narrow peaks of the column 2 separation to provide a true enhancement in peak capacity production going from 1D-GC to GC × GC. Hence, the GC × GC design we report has not had the primary separation peaks purposely broadened in order to allow longer modulation periods (e.g., several seconds instead of the 200 ms used herein), as is the common practice. The instrumental approach reported herein provides a concurrent selectivity advantage for GC × GC over 1D-GC, and a peak capacity production advantage. The incentive to reduce off-column band broadening in GC technology is ever more apparent. The benefits of addressing this issue are significant.

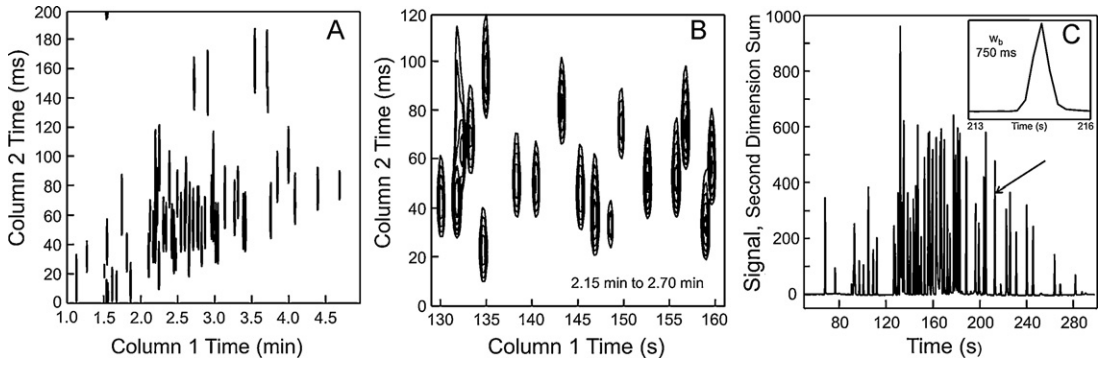

Fig. 8. (A) GC × GC-FID chromatogram of the test mixture defined in Table 1 utilizing a 40 m × 180 μm Rtx-5 column for column 1, and a 2 m × 100 μm i.d. ionic liquid column for column 2. After a 0.8 min delay post-injection to column 1, the modulator valve onto column 2 was activated, making 15 ms injection pulses every 200 ms. The absolute head pressure on column 1 was programmed from 517 kPa to 793 kPa during the temperature program. The absolute head pressure on column 2 was held constant at 621 kPa. (B) Detailed view of the peaks clustered between 126 s and 162 s. (C) 1D representation of A, the result of summing the entire signal collected for column 2 onto the first dimension.

5. Conclusion

By reducing band broadening due to injection, substantially improved peak capacity production was achieved using a commercial GC instrument platform. Increased peak capacity production allows the analysis time to decrease if the total peak capacity is held constant to address a particular analysis challenge, making these findings particularly useful in applications requiring high throughput. These benefits were extended to GC × GC. The experimental findings were also consistent with the band broadening theory presented herein. Future advances in injection and detection technology are warranted to further advance these benefits and bring these approaches into the hands of the general practitioner.

Acknowledgment

This report is based upon work supported in part by DARPA under subcontracts through Honeywell Laboratories and SRI International from contract HR0011-09-C-0049. The views and conclusions contained in this document are those of the authors and should not be interpreted as representing the official policies, either expressed or implied, of the Defense Advanced Research Projects Agency or the U.S. Government. The third-party trademarks used herein are trademarks of their respective owners. Helpful discussions with A.D. McBrady of Honeywell are gratefully acknowledged. The authors thank D.W. Armstrong and co-workers for supplying the ionic liquid column used in the GC × GC studies.

References

[1] J.C. Giddings, Anal. Chem. 39 (1967) 1027.
[2] J.L. Hope, K.J. Johnson, M.A. Cavelti, B.J. Prazen, J.W. Grate, R.E. Synovec, Anal. Chim. Acta 490 (2003) 223.
[3] G.M. Gross, B.J. Prazen, J.W. Grate, R.E. Synovec, Anal. Chem. 76 (2004) 3517.
[4] V.R. Reid, A.D. McBrady, R.E. Synovec, J. Chromatogr. A 1148 (2007) 236.
[5] A. Peters, M. Klemp, L. Puig, C. Rankin, R. Sacks, Analyst 116 (1991) 1313.
[6] F. Xu, W. Guan, G. Yao, Y. Guan, J. Chromatogr. A 1186 (2008) 183.
[7] C. Leonard, A. Grall, R. Sacks, Anal. Chem. 71 (1999) 2123.
[8] V.R. Reid, R.E. Synovec, Talanta 76 (2008) 703.
[9] Z. Liu, S.R. Sirimanne, D.G. Patterson, L.L. Needham, J.B. Phillips, Anal. Chem. 66 (1994) 3086.
[10] D. Stajnbaher, L. Zupancic-Kralj, J. Chromatogr. A 1015 (2003) 185.
[11] H. Yan, F. Qiao, M. Tian, K.H. Row, J. Pharm. Biomed. Anal. 51 (2010) 774.
[12] V. Wulf, N. Wienand, M. Wirtz, H. Kling, S. Gäb, O.J. Schmitz, J. Chromatogr. A 1217 (2010) 749.
[13] V. Matamoros, E. Jover, J.M. Bayona, Anal. Chem. 82 (2010) 699.
[14] Z. Liu, J.B. Phillips, J. Chromatogr. Sci. 29 (1991) 227.
[15] L.M. Blumberg, F. David, M.S. Klee, P. Sandra, J. Chromatogr. A 1188 (2008) 2.
[16] A.E. Sinha, B.J. Prazen, C.G. Fraga, R.E. Synovec, J. Chromatogr. A 1019 (2003) 79.
[17] W.C. Siegler, J.A. Crank, D.W. Armstrong, R.E. Synovec, J. Chromatogr. A 1217 (2010) 3144.
[18] G. Guiochon, Anal. Chem. 38 (1966) 1020.
[19] D.R. Lide, CRC Handbook of Chemistry and Physics, CRC Press, 2004.
[20] A.E. Sinha, K.J. Johnson, B.J. Prazen, S.V. Lucas, C.G. Fraga, R.E. Synovec, J. Chromatogr. A 983 (2003) 195.
[21] T. Payagala, Y. Zhang, E. Wanigasekara, K. Huang, Z.S. Breitbach, P.S. Sharma, L.M. Sidisky, D.W. Armstrong, Anal. Chem. 81 (2009) 160.